J Eng Math (2010) 67:71–84
DOI 10.1007/s10665-009-9328-5

Dispersive nonlinear shallow-water equations: some preliminary numerical results

Giovanna Grosso · Matteo Antuono · Maurizio Brocchini

Received: 30 December 2008 / Accepted: 31 August 2009 / Published online: 15 September 2009

Abstract The dispersive nonlinear shallow-water equations of Antuono et al. (Stud Appl Math 122:1–28, 2008) are solved by means of an explicit arbitrary high-order accurate finite-volume scheme for nonlinear hyperbolic systems with stiff source terms. Tests against typical benchmark solutions are used to illustrate the robustness and accuracy of the solver while typical solutions for the propagation of solitary waves on a slope highlight the solution value in reproducing nearshore flows.

Keywords Boussinesq equations · Dispersive nonlinear shallow-water equations · Finite-volume solvers · Nearshore · Nonlinear shallow-water equations · Waves

1 Introduction

The mathematical and numerical modeling of nearshore flows has grown enormously in the last 30–40 years. It is becoming more and more evident that the pioneering contributions given by Professor DH Peregrine to this research field, which provides the needed bases both to shallow-water oceanographic studies and to coastal-engineering analyses, have been fundamental. His studies of wave propagation in shallow water laid the foundations of a major part of modern nearshore hydrodynamics.

The impact of the paper "Long waves on a beach" [1] goes well beyond the 340 official citations it currently counts: virtually all modern Boussinesq-type models for dispersive waves on shallow waters derive theoretical and numerical rationales from that paper which introduced equations which might deserve to be named "Peregrine's equations".

A similarly important influence has been Professor Peregrine's contribution to the modeling of nearshore flows by means of the Nonlinear Shallow-Water Equations (NSWEs hereinafter). The work of Hibberd and Peregrine

G. Grosso
DICAT, Università di Genova, via Montallegro 1, 16145 Genova, Italy
e-mail: ggrosso@dicat.unige.it

M. Antuono
INSEAN (The Italian Ship Model Basin), via di Vallerano 139, 00128 Rome, Italy

M. Brocchini (✉)
Dipartimento ISAC, Università Politecnica delle Marche, via Brecce Bianche 12, 60131 Ancona, Italy
e-mail: m.brocchini@univpm.it

[2] "Surf and run-up on a beach: a uniform bore", co-authored with his PhD student Stephen Hibberd, has both opened the way to the modern approach of solving the NSWE by means of Godunov-type models and solved the long-standing problems associated with the numerical representation of the shoreline motion induced by breaking waves.

In view of the above, we are honored to provide a contribution to the research field which Professor Peregrine so extensively enriched by illustrating some solutions of a model aimed at reconciling and integrating the approaches based on both NSWEs and Boussinesq-type equations (BTEs hereinafter).

The model in question is based on Dispersive Nonlinear Shallow-Water Equations (DNSWEs hereinafter) and has been conceived to overcome some of the theoretical and numerical limits associated with both NSWEs and BTEs.

In more detail, the fundamental limitations introduced by the BTEs are related with the treatment of the shoreline boundary conditions and with the representation of wave-breaking-induced energy dissipation while the NSWEs are largely limited by the poor representation of wave shoaling.

Problems also arise in the numerical solution of the chosen model equations; this is particularly true for the BTEs; the development of suitable numerical methods has lagged behind the effort devoted to finding the most suitable set of equations. Recent studies have recognized a need to treat the nonlinear and dispersive operators separately, each with the most suitable numerical method. Some of these models, based on the Operator Splitting approach [3,4] were also "hybrid" in terms of the numerical techniques in use. For example, Erduran et al. [5] used a finite-volume method for the conservative part of the equations while the highest-order dispersive terms were discretized using a finite-difference scheme. All these methods provide fairly good predictions at the cost of using varied numerical schemes with different characteristics. More recently Cienfuegos et al. [6] chose a Godunov-type solver for the whole weakly dispersive BTEs at hand, thus employing numerical techniques typically employed in the solution of the NSWEs to integrate a set of BTEs.

The approach illustrated in the present paper is radically new: a set of DNSWEs is used to allow both a theoretically sound description of the dispersive terms absent in the NSWEs and an efficient numerical solution by means of finite-volume techniques, the best suited for the NSWEs.

The model equations are briefly described in Sect. 2, while Sect. 3 gives a more detailed account of the numerical approach in use. Results aimed at a preliminary validation of the numerical solver and useful to illustrate the main features of numerical solutions for waves propagating on a beach are summarized in Sect. 4. This also provides a short discussion of the research activities underway to improve the practical features of the model (e.g., shoaling).

2 The DNSWEs

2.1 Background

For the analyses which follow, we define the scaling needed to pass from dimensional (starred) to dimensionless (non-starred) variables (see also Fig. 1). In the region in which the bed is approximately horizontal ($h^* \simeq$ const.) it reads:

$$x^* = x_0^* x = \frac{x}{k^*}, \quad \eta^* = d_0^* \eta, \quad t^* = \frac{t}{k^* \sqrt{g d_0^*}}, \quad u^* = \sqrt{g d_0^*}\, u, \quad h^* = d_0^* h, \tag{1}$$

where $k^* = 2\pi/L^*$, L^* is the wave length, d_0^* is a scale for the water depth (here taken as the offshore still-water depth), g is the gravity acceleration. We also define the (dimensionless) dispersion coefficient $\mu = k^* d_0^*$ and the (dimensionless) nonlinearity parameter $\epsilon = H_0^*/d_0^*$ where H_0^* is the wave amplitude. As a consequence, the order of magnitude of η (as well as u) is $\mathcal{O}(\epsilon)$.

To illustrate all the details of our analysis we refer to a specific set of BTEs chosen (see also [7], `ALB08` in the following, and [8]) because it is:

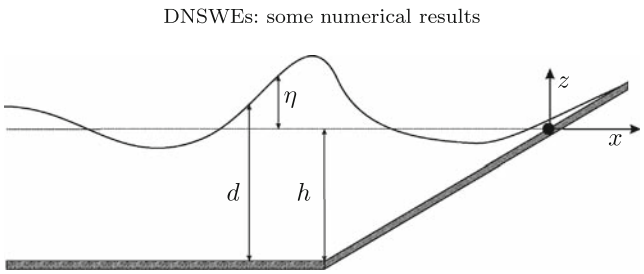

Fig. 1 Sketch of geometry and flow dimensionless variables for the beach problem

– (1)physically sound and complete and (2) has practical applicability. First of all, it has been derived without assuming the flow to be irrotational, hence it can intrinsically handle rotational and breaking waves, this being an essential feature of any model wishing to represent real-life nearshore flows;
– (3)theoretically well posed and (4) can be effectively solved. The model is weakly nonlinear and weakly dispersive, hence, though being rather simple and of compact form, it retains all the fundamental properties of the class of models we want to study.

Following ALB08 we refer to the following $\mathcal{O}(\mu^4, \epsilon\mu^2)$-accurate model equations (typical of a weakly nonlinear BTEs model):

$$\eta_t + Q_x = 0, \quad Q_t + \left(\frac{d^2}{2} + \frac{Q^2}{d}\right)_x - \mu^2 d^2 \left[\frac{d}{3} u_{xxt} + d_x u_{xt} + \frac{h_{xx}}{2} u_t\right] = h_x d, \tag{2}$$

in which u is the onshore velocity, η is the free-surface location, $h = h(x)$ is the still-water depth, $d = h + \eta$ is the total water depth and $Q \equiv ud$.

These extend those of [8] to properly describe frequency dispersion also in the very shallow near-shoreline waters (see ALB08 and [9]).

As a first step towards achieving a hyperbolic approximation of the above model equations, ALB08 performed some pre-conditioning of the $O(\mu^2)$-dispersive terms. Such a procedure can, in principle, be applied to more complicated BTEs (like fully nonlinear and fully dispersive) the price being a major practical difficulty of handling the large amount of high-order terms involved. In this respect the chosen model has the merits of providing, at a reasonably reduced cost, both a physically sound description of the nearshore dynamics and a complete representation of dispersive and nonlinear phenomena.

After some algebra, and in the presence of bathymetry smooth enough that both $|h_{xx}| \ll 1$ and $h_x^2/3 \ll 1$, the following dimensional system of model equations is achieved (see ALB08 for details):

$$d_t + Q_x = 0, \quad Q_t + \left(\frac{d^2}{2} + \frac{Q^2}{d} - \mu^2 \frac{d^2 Q_{xt}}{3}\right)_x = h_x d \left(1 - \mu^2 \frac{Q_{xt}}{3}\right). \tag{3}$$

The accuracy of the system (3) is still $\mathcal{O}(\mu^4, \epsilon\mu^2)$ but, differently from the original system of [8], it satisfies the following conditions:

1. the approximated dispersive terms account for the main dispersive mechanisms over the entire nearshore;
2. such dispersive terms tend to zero as d tends to zero;
3. they can be written in conservative form when the hyperbolic approximation is applied.

The latter condition is needed to apply the hyperbolic approximation described in the next section and, consequently, to get correct shock relations.

2.2 The model equations

Apart from the terms depending on Q_{xt}, system (3) is very similar to a quasi-linear set of hyperbolic equations. Hence, solution of this set can make the most of all the results (mathematical and numerical) available for this class

of equations. Thus, a mathematical procedure which enables rewriting the DNSWEs as a hyperbolic quasi-linear systems avoids all the numerical problems arising when modeling the dispersive BTEs terms. Hence, our aim is to introduce variables and equations suited to rewrite the previous system as a hyperbolic quasi-linear system. We call such a procedure a hyperbolic approximation of the BTEs. In the following we first define the hyperbolic approximation based on a time-average procedure and, then, extend it in a general way.

2.2.1 Physical interpretation

A simple physical interpretation of the proposed model is suggested here: the hyperbolic model can be derived by an averaging procedure. Consider the dimensionless system (3) as a starting model of accuracy $\mathcal{O}(\epsilon\mu^2, \mu^4)$ and, for the sake of simplicity, assume h = constant. We, then, define the following averaging operator:

$$\bar{f}(t;x) = \frac{1}{2\tau}\int_{t-\tau}^{t+\tau} f(s;x)\,\mathrm{d}s. \tag{4}$$

The time scale τ is fixed and is assumed to be small enough.

By averaging, introducing the pseudo-potential function $\psi = \eta_{tt}$, neglecting the high-order terms and using the continuity equation, the system (3) becomes (see ALB08 for details):

$$\bar{\eta}_t + \overline{Q}_x = 0, \quad \overline{Q}_t + \left(\frac{\bar{d}^2}{2} + \frac{\overline{Q}^2}{\bar{d}} + \frac{\mu^2}{3}\bar{d}^2\psi\right)_x = 0, \quad \frac{\tau^2}{6}\psi_{tt} + \psi + \bar{Q}_{xt} = 0. \tag{5}$$

It is simple to show that system (5) is both hyperbolic and dispersive. Moreover, choosing τ^2 proportional to μ^2, it has the same order of accuracy of the original non-hyperbolic model (3). This means that (5) is not only the hyperbolic approximation of the second-order shallow-water equations, but it can be considered as the dispersive shallow-water model in its own right.

2.2.2 A hyperbolic approximation

The generalization of the averaging procedure of the previous section can be achieved through use of two pseudo-potential functions. We first assume the existence of a new variable ψ^* enabling the substitution:

$$Q^*_{x^*t^*} \longrightarrow Q^*_{x^*t^*} + \gamma\psi^*_{t^*t^*}, \tag{6}$$

in which γ is a positive dimensionless parameter (such a hypothesis implies $[\psi^*]$ has the dimensions of a length, i.e., $[\psi^*] = \mathrm{L}$). To obtain an approximation "near" to the starting set of the dispersive equations, we assume $\gamma \ll 1$ and impose ψ^* to obey the constitutive equation:

$$-A^*\psi^* = Q^*_{x^*t^*} + \gamma\psi^*_{t^*t^*}, \tag{7}$$

in which A^* is a *positive* dimensional parameter ($[A^*] = \mathrm{T}^{-2}$). Under specific initial conditions (see ALB08 for details), Eq. 7 enables ψ^* to approximate $Q^*_{x^*t^*}$ for $\gamma \ll 1$. Defining $\psi^* = \psi_0\psi$ and balancing (7) (the leading term is $Q^*_{x^*t^*}$), we have $\psi_0 = \mu^2 g/A^*$ in accordance with the scaling in use. Conversely, A^* must not depend on the scaling; then a possible choice is $A^* = ag/d_0^*$ in which a is a *positive* dimensionless number used to "normalize" the value of A^* (i.e., we can always assume $A^* = 1\mathrm{s}^{-2}$ with no loss of generality). To write the system in the canonical conservative format, we introduce the pseudo-potential ϕ^* such that $\phi^*_{t^*} = \psi^*$. Defining $\phi^* = \phi^*_0\phi$ and balancing the previous equation, we obtain the following scale relationship: $\phi^*_0 = \psi^*_0 t^*_0$. Using the results obtained above, we, finally, get the dimensionless DNSWEs:

$$d_t + Q_x = 0, \quad Q_t + \left(\frac{d^2}{2} + \frac{Q^2}{d} + \mu^2\frac{d^2}{3}\psi\right)_x = h_x d\left(1 + \mu^2\frac{\psi}{3}\right), \quad \phi_t = \psi, \quad \gamma\frac{\mu^2}{a}\psi_t + Q_x = -\phi. \tag{8}$$

Note that if h = constant, the system (8) reduces to (5). In this case, we get $\tau^2/6 = \mu^2\gamma/a$.

3 The solution method

The DNSWEs (8) can be written in the typical general form used for hyperbolic systems of conservation laws:

$$\left.\begin{array}{l}\text{PDEs} : \mathbf{u}_t + \mathbf{f}(\mathbf{u})_x = \mathbf{S}(\mathbf{u}), \\ \text{ICs} \quad : \mathbf{u}(x,0) = \mathbf{u}_0(x).\end{array}\right\} \tag{9}$$

Since the dissipative/productive process, associated with the source term of system (9), is much faster than the conservative one, associated with the homogeneous part of the equations, the source term is said to be "stiff" and appropriate algorithms are required for its solution.

By integrating the system of balance laws (9) over a finite space–time control volume, the finite-volume formulation can be obtained, which reads

$$\bar{\mathbf{u}}_i^{n+1} = \bar{\mathbf{u}}_i^n - \frac{\Delta t}{\Delta x_i}\left(\mathbf{f}_{i+\frac{1}{2}} - \mathbf{f}_{i-\frac{1}{2}}\right) + \Delta t \bar{\mathbf{S}}_i. \tag{10}$$

A numerical flux and a numerical source term have to be chosen, such that the numerical scheme is consistent, stable and accurate. Moreover, the scheme has to be well-balanced, robust (even on coarse grids) and asymptotically consistent.

A wealth of methods to solve numerically systems of balance laws with stiff source terms is available in the literature. The best schemes are well-balanced and asymptotically consistent, but the only one that can reach any order of accuracy in space and time under standard CFL stability conditions is the one proposed by Dumbser et al. [10]. We have chosen such a scheme to solve the DNSWEs. We here provide a synthetic, though complete, description of the method, mainly focussing on the steps needed to apply it to the specific problem here at hand, i.e., the DNSWEs. More details on the numerical technique can be found in [10].

3.1 An explicit, arbitrary high-order accurate, finite-volume scheme for nonlinear hyperbolic systems with stiff source terms

In this section we briefly summarize the method of [10] and describe its application to the DNSWEs.

The spatial computational domain $\Omega \in I\!R$ is completely covered by pairwise disjoint spatial elements $Q_i =]x_{i-\frac{1}{2}}; x_{i+\frac{1}{2}}[$, with $\Delta x_i = x_{i+\frac{1}{2}} - x_{i-\frac{1}{2}}$ and the cell average of $\mathbf{u}(x,t)$ within Q_i at the time t^n is defined as

$$\bar{\mathbf{u}}_i^n = \frac{1}{\Delta x_i}\int_{x_{i-\frac{1}{2}}}^{x_{i+\frac{1}{2}}} \mathbf{u}(x,t^n)\mathrm{d}x. \tag{11}$$

For all the computations which follow, we assume $\Delta x_i = \Delta x = \text{const}$. The time step $\Delta t = t^{n+1} - t^n$ together with the spatial element Q_i generate the space–time element $\mathbb{Q}_i = Q_i \times]t^n; t^n + \Delta t[$. Within one element $\mathbb{Q}_i$, local space- and time-coordinates are defined, such as $0 \le \xi \le 1$ and $0 \le \tau \le 1$. They are associated with the global coordinates x and t by the relations

$$x = x_{i-\frac{1}{2}} + \xi \Delta x_i \quad \text{and} \quad t = t^n + \tau \Delta t. \tag{12}$$

The standard finite-volume discretization (10) of the system (9) is given, where

$$\mathbf{f}_{i+\frac{1}{2}} = \int_0^1 \mathbf{f}_h(\mathbf{u}_i(1,\tau), \mathbf{u}_{i+1}(0,\tau))\mathrm{d}\tau \quad \text{and} \quad \bar{\mathbf{S}}_i = \int_0^1\int_0^1 \mathbf{S}(\mathbf{u}_i(\xi,\tau))\mathrm{d}\xi\,\mathrm{d}\tau, \tag{13}$$

where $\mathbf{f}_h(\mathbf{u}_i(1,\tau), \mathbf{u}_{i+1}(0,\tau))$ denotes a numerical flux function depending on the two arguments $\mathbf{u}_i(1,\tau)$ and $\mathbf{u}_{i+1}(0,\tau)$, which are the boundary extrapolated data on the left and on the right side of the element interface $i + \frac{1}{2}$.

As described in detail in the following, the steps needed to construct an arbitrary high-order essentially non-oscillatory explicit one-step finite-volume scheme are: (I) nonlinear (non-oscillatory) reconstruction of spatial polynomials from the given cell averages at time t^n, (II) local solution of the initial-value problem (9) inside each element, where the initial data are given by the spatial reconstruction polynomial at time t^n, (III) numerical integration of integrals in (13) and update of the cell averages according to (10).

3.1.1 The nonlinear reconstruction

In the following we briefly describe the proposed nonlinear weighted essentially non-oscillatory (WENO) reconstruction procedure used to reconstruct higher-order polynomial data within each spatial cell Q_i at time t^n from the given cell averages $\bar{\mathbf{u}}_i^n$.

The reconstruction procedure follows directly form the procedure suggested in [11] for general unstructured two- and three-dimensional meshes.

Reconstruction is done for each element on a stencil S_i^s, which is given by the following union of the element Q_i and its neighbors Q_j:

$$S_i^s = \bigcup_{j=i+s-k}^{i+s+k} Q_j, \tag{14}$$

where s is the stencil shift with respect to the central element Q_i and k is the spatial extension of the stencil to the left and to the right. In this approach three fixed reconstruction stencils are always used: S_i^0, S_i^{-k} and S_i^k. Given the cell-average data $\bar{\mathbf{u}}_i^n$ in all elements Q_i, we want to obtain a spatial reconstruction polynomial at time t^n, in the form

$$\mathbf{w}_i^s(\xi, t^n) = \sum_{l=0}^{M} \psi_l(\xi)\hat{\mathbf{w}}_l^{(i,s)}(t^n) = \psi_l(\xi)\hat{\mathbf{w}}_l^{(i,s)}(t^n), \tag{15}$$

where (the last step only recalls that summation is made for repeated indices) we use the rescaled Legendre polynomials for the spatial reconstruction basis functions $\psi_l(\xi)$, such that the $\psi_l(\xi)$ form an orthogonal basis on the unit interval $I = [0; 1]$. The number of polynomial coefficients (degrees of freedom) is $L = M + 1$, where M is the degree of the reconstruction polynomial. To compute the reconstruction polynomial $\mathbf{w}_i(\xi, t^n)$ valid for the element Q_i, we require integral conservation for all elements Q_j inside the stencil S_i^s, i.e.,

$$\int_{Q_j} \mathbf{w}_i^s(\xi, t^n)\mathrm{d}\xi = \int_{Q_j} \Psi_l(\xi)\mathrm{d}\xi\,\hat{\mathbf{w}}_l^{(i,s)}(t^n) = \bar{\mathbf{u}}_j^n, \quad \forall Q_j \in S_i^s. \tag{16}$$

Equation 16 yields a linear equation system of the form

$$A_{j,l}\hat{\mathbf{w}}_l^{(i,s)}(t^n) = \bar{\mathbf{u}}_j^n \tag{17}$$

for the unknown coefficients $\hat{\mathbf{w}}_l^{(i,s)}(t^n)$ of the reconstruction polynomial on the stencil S_i^s. Since we choose $k = M/2$ for even values of M and $K = (M + 1)/2$ for odd values of M, the number of elements in S_i^s may become larger than the number of degrees of freedom L. In this case, we can use a constrained least-squares technique according to [11] to solve (17).

To obtain the final non-oscillatory reconstruction polynomials for each Q_i at time t^n, we finally construct a data-dependent nonlinear combination of the polynomials $\mathbf{w}_i^0(\xi, t^n)$, $\mathbf{w}_i^{-k}(\xi, t^n)$ and $\mathbf{w}_i^k(\xi, t^n)$ obtained from the central, left-sided and right-sided stencils as follows:

$$\mathbf{w}_i(\xi, t^n) = \hat{\mathbf{w}}_l^i(t^n)\Psi_l(\xi), \tag{18}$$

with

$$\hat{\mathbf{w}}_l^i(t^n) = \omega_0\hat{\mathbf{w}}_i^0(\xi, t^n) + \omega_{-k}\hat{\mathbf{w}}_i^{-k}(\xi, t^n) + \omega_k\hat{\mathbf{w}}_i^k(\xi, t^n). \tag{19}$$

The expressions for the nonlinear weights ω_s can be found in [11]. These weights are such that the proposed reconstruction typically uses the accurate and linearly stable central-stencil reconstruction in those regions where the solution is smooth. However, in the presence of discontinuities, the smoother left- or right-sided stencils are preferred, as for standard ENO and WENO methods.

For nonlinear hyperbolic systems, the reconstruction should be made using characteristic variables (see [11,12]) in order to avoid spurious oscillations that may appear when applying ENO or WENO reconstruction operators component-wise to nonlinear hyperbolic systems.

After the reconstruction procedure, we get a non-oscillatory spatial polynomial $\mathbf{w}_i^s(\xi, t^n)$ defined at time t^n inside each spatial element Q_i. However, in order to compute the integrals in (13), we need to compute the temporal evolution of these polynomials inside each space–time element $\mathbb{Q}_i$ in order to be able to compute the integrals appearing in (13).

Since it is a well-known fact that methods based on Taylor series usually do not work in the presence of stiff source terms, Dumbser et al. [10] propose to replace the Cauchy–Kovalewsky procedure, generally used for the temporal evolution of the reconstruction polynomial, by a new local space–time Discontinuous Galerkin (DG) scheme.

3.1.2 The local space–time Discontinuous Galerkin scheme

In the following, we briefly illustrate the local space–time DG scheme of [10].

The space of basis and test functions V_h of the local space–time DG scheme is defined as the space spanned by piecewise polynomials given by the space–time tensor products of the scaled Legendre polynomials $\psi_i(\xi)$ and $\psi_j(\tau)$ of degree $0 \leq i, j \leq M$, i.e.,

$$\phi_k = \phi_k(\xi, \tau) = \psi_i(\xi) \otimes \psi_j(\tau), \tag{20}$$

where $1 \leq k = k(i, j) \leq N_d$, with $N_d = (M+1)^2$. The local numerical solution of (9) u_p^i, inside each space–time control volume $\mathrm{d}Q_i$, is approximated within the reference element $\mathbb{Q}_E = [0; 1]$ using the basis functions ϕ_k, i.e.,

$$u_p^i(\xi, \tau) = \sum_{l=1}^{N_d} \phi_l(\xi, \tau) \hat{u}_l^i = \phi_l(\xi, \tau) \hat{u}_{pl}^i. \tag{21}$$

Moreover, the following two scalar products of two functions $f(\xi, \tau)$ and $g(\xi, \tau)$ are defined

$$\langle f, g \rangle = \int_0^1 \int_0^1 f(\xi, \tau) g(\xi, \tau) \mathrm{d}\xi \mathrm{d}\tau, \quad [f, g] = \int_0^1 f(\xi, \tau) g(\xi, \tau) \mathrm{d}\xi. \tag{22}$$

In order to obtain the proposed local space–time DG finite-element method for general nonlinear hyperbolic systems of conservation laws with source terms, the system (9) is re-written in local coordinates of the reference element

$$\frac{\partial}{\partial \tau} \mathbf{u} + \frac{\partial}{\partial \xi} \mathbf{f}^*(\mathbf{u}) = \mathbf{S}^*(\mathbf{u}), \tag{23}$$

where $\mathbf{f}^*(\mathbf{u}) = \Delta t \xi_x \mathbf{f}(\mathbf{u})$ and $\mathbf{S}^*(\mathbf{u}) = \Delta t \mathbf{S}(\mathbf{u})$. Hence, the modified governing equations are multiplied by the test functions ϕ_k and integrated over the reference element $\mathbb{Q}_E$. In order to keep a local formulation, which does not need any information from the neighbor elements, the integration by parts is used only in time; it gives

$$[\phi_k(\xi, 1), \mathbf{u}(\xi, 1)] - [\phi_k(\xi, 0), \mathbf{u}(\xi, 0)] - \left\langle \frac{\partial}{\partial \tau} \phi_k, \mathbf{u} \right\rangle + \left\langle \phi_k, \frac{\partial}{\partial \xi} \mathbf{f}^*(\mathbf{u}) \right\rangle = \langle \phi_k, \mathbf{S}^*(\mathbf{u}) \rangle. \tag{24}$$

The initial condition is given by the reconstruction polynomials obtained from the reconstruction operator applied to the cell averages at the current time t^n. Using the time fluxes and the *ansatz* (21) for the numerical solution, we obtain

$$[\phi_k(\xi, 1), \phi_l(\xi, 1)] \hat{\mathbf{u}}_l^i - [\phi_k(\xi, 0), \psi_m(\xi)] \hat{\mathbf{w}}_m^i(t^n) - \left\langle \frac{\partial}{\partial \tau} \phi_k, \phi_l \right\rangle \hat{\mathbf{u}}_l^i + \left\langle \phi_k, \frac{\partial}{\partial \xi} \mathbf{f}^*(\phi_l \hat{\mathbf{u}}_l^i) \right\rangle = \left\langle \phi_k, \mathbf{S}^*(\phi_l \hat{\mathbf{u}}_l^i) \right\rangle. \tag{25}$$

In order to solve the local nonlinear set of equations (25), it is necessary to use an algorithm for finding roots of nonlinear equation systems, for instance the Newton method. The strategy suggested by Dumbser et al. [10] is based on the following steps:

1. the nonlinear system (25) is linearized with respect to the initial condition given by $\mathbf{W}^i(\xi, t^n)$;
2. the resulting linear equation system is solved exactly using Gauss–Jordan elimination and an initial guess $\hat{\mathbf{U}}_l^{(i,1)}$ of the solution $\hat{\mathbf{U}}_l^i$ is obtained;
3. a new linearization of the system (25) about $\hat{\mathbf{U}}_l^{(i,1)}\phi_l(\xi, 1)$ is performed and the resulting linear system is solved producing a second guessed value $\hat{\mathbf{U}}_l^{(i,2)}$;
4. this procedure is, usually, repeated three times and the third guessed value $\hat{\mathbf{U}}_l^{(i,1)}$ is the starting point of a standard multivariate Newton method for nonlinear systems of equations.

Once the solution $\bar{\mathbf{u}}_l^i$ of the local space–time DG method (25) is known, it is possible to use the solution $\mathbf{u}_i(\xi, \tau) = \Phi_l(\xi, \tau)\hat{\mathbf{u}}_l^i$ to compute the arguments for the source term and the numerical flux in (13) that are needed for the explicit finite-volume scheme (10). The integral appearing in (13) are computed using classical Gaussian quadrature formulae; see, e.g., [13] for details.

3.2 A well-balanced scheme

Standard methods that correctly solve systems of conservation laws can fail when approaching equilibria or near equilibria solutions. In the context of shallow-water equations, Bermúdez et al. [14] introduced the condition called "conservation property": a scheme is said to satisfy this condition if it correctly solves the steady-state solutions corresponding to water at rest. This idea of constructing numerical schemes that preserve some equilibria, which are called in general well-balanced schemes has been extended in different ways; in particular, the work developed by Castro et al. [15] provides a general expression for a well-balanced high-order method, based on the use of a first-order Roe scheme and reconstruction of states. From such a general expression, specific schemes can be deduced for any system of balance laws, and in such a way that the numerical treatments of the terms (for sources and for coupling) are derived automatically. For this reason, such a method can be easily applied also to the explicit arbitrarily high-order accurate finite-volume scheme for nonlinear hyperbolic systems with stiff source terms of [10].

To use the procedure suggested by [15], the generic hyperbolic system of balance laws

$$\frac{\partial}{\partial t}\mathbf{u} + \frac{\partial}{\partial x}\mathbf{f}(\mathbf{u}) = \mathbf{S}(\mathbf{u})\frac{\partial \sigma}{\partial x}, \tag{26}$$

where $\sigma(x)$ is a known function from $\mathbb{R}$ to $\mathbb{R}$, must be rewritten as an extended quasi-linear non-conservative system:

$$\frac{\partial \mathbf{u}}{\partial t} + \mathbf{A}(\mathbf{u})\frac{\partial \mathbf{u}}{\partial x} = 0, \quad x \in \mathbb{R}, t > 0, \tag{27}$$

after adding to (26) the trivial equation

$$\frac{\partial \sigma}{\partial t} = 0. \tag{28}$$

The term $\frac{\partial \sigma}{\partial x}$ in (26) represents the x-derivative of a generic function (of the x-variable, only), which can be present in the system, and which can lead to numerical integration problems. In the specific case in hand, such a term represents the x-derivative of the still-water depth, which accounts for bed variations (and it does not depend on time in a fixed-bed approximation).

Then, by introducing a family of paths Ψ and a Roe linearization $\mathcal{A}_\Psi$ of system (27), the explicit arbitrary high-order accurate finite-volume scheme for nonlinear hyperbolic systems with stiff source terms of [10] can be easily made to be well-balanced. In particular, the update formula for (26) becomes:

$$\mathbf{u}_i^{n+1} = \mathbf{u}_i^n - \frac{\Delta t}{\Delta x}(\mathbf{f}_{i+\frac{1}{2}} - \mathbf{f}_{i-\frac{1}{2}} + \mathbf{A}_i), \tag{29}$$

where

$$\mathbf{f}_{i+\frac{1}{2}} = \int_{t^n}^{t^{n+1}} \mathbf{A}^-_{i+\frac{1}{2}}(\mathbf{u}^+_{i+\frac{1}{2}}(t) - \mathbf{u}^-_{i+\frac{1}{2}}(t))\mathrm{d}t, \tag{30}$$

$$\mathbf{f}_{i-\frac{1}{2}} = -\int_{t^n}^{t^{n+1}} \mathbf{A}^+_{i-\frac{1}{2}}(\mathbf{u}^+_{i-\frac{1}{2}}(t) - \mathbf{u}^-_{i-\frac{1}{2}}(t))\mathrm{d}t \tag{31}$$

and

$$\mathbf{A}_i = \int_{x_{i-\frac{1}{2}}}^{x_{i+\frac{1}{2}}} \int_{t^n}^{t^{n+1}} \mathbf{A}(\mathbf{u}_i(x,t))\frac{\mathrm{d}}{\mathrm{d}x}\mathbf{u}_i(x,t))\mathrm{d}x\mathrm{d}t. \tag{32}$$

Here the intermediate matrices are defined by

$$\mathbf{A}_{i+\frac{1}{2}} = \mathbf{A}_\Psi(\mathbf{U}^n_i, \mathbf{U}^n_{i+1}) \tag{33}$$

and

$$\mathcal{L}^\pm_{i+\frac{1}{2}} = \begin{bmatrix} (\lambda_1^{i+\frac{1}{2}})^\pm & \dots & 0 \\ \vdots & \ddots & \vdots \\ 0 & \dots & (\lambda_N^{i+\frac{1}{2}})^\pm \end{bmatrix}, \quad \mathbf{A}^\pm_{i+\frac{1}{2}} = \mathcal{K}_{i+\frac{1}{2}}\mathcal{L}^\pm_{i+\frac{1}{2}}\mathcal{K}^{-1}_{i+\frac{1}{2}}, \tag{34}$$

where $\mathcal{L}_{i+\frac{1}{2}}$ is the diagonal matrix whose coefficients are the eigenvalues of $\mathbf{A}_{i+\frac{1}{2}}$:

$$\lambda_1^{i+\frac{1}{2}} < \lambda_2^{i+\frac{1}{2}} < \dots < \lambda_N^{i+\frac{1}{2}}, \tag{35}$$

and $\mathcal{K}_{i+\frac{1}{2}}$ is a $N \times N$ matrix whose columns are the associated eigenvectors. Moreover, the arguments $\mathbf{u}_i(x,t)$ for the numerical fluxes in (30) and (31) and for the matrix $\mathcal{A}$ in (32) are given by the solution $\mathbf{u}_i(\xi,\tau) = \Phi_l(\xi,\tau)\hat{\mathbf{u}}^i_l$, obtained by solving the local space–time DG method (25). For the sake of simplicity, the simplest family of paths can be chosen, i.e., the family of segments (see [15]). It can be shown [16] that the method (29) based on the family of segments is well-balanced at least with order 2.

4 Some results

In the following two subsections some results are shown which illustrate the potential of the equations in use and the quality of the wave-type solutions of the DNSWEs.

4.1 A fundamental solution

The DNSWEs have an analytical solution in the form of solitary waves over a horizontal bed. Such a solution represents a good benchmark for the numerical one, as a direct comparison can be easily made between the two. The procedure for calculating the analytical solitary-wave solution can be found in `ALB08`. To test the numerical propagation of the solitary-wave solution of the DNSWEs, we need to write such an analytical solution as an appropriate initial condition for the model. In particular, we need:

$$\begin{aligned} d_0(x) &= d(x, t=0), \quad Q_0(x) = Q(x, t=0), \\ \phi_0(x) &= \phi(x, t=0), \quad \psi_0(x) = \psi(x, t=0). \end{aligned} \tag{36}$$

To get the initial data we have to solve the following Ordinary Differential Equation (ODE) (see ALB08)

$$\left(\frac{\mathrm{d}d}{\mathrm{d}x}\right)^2 = \frac{2}{\mathrm{Fr}^2(\hat{\gamma}\,\hat{w}(d)-1)^2}\left\{3\left[\frac{\mathrm{Fr}^2}{2d^2}-\frac{1+2\mathrm{Fr}^2}{2\,d}-\frac{d}{2}+1+\frac{\mathrm{Fr}^2}{2}\right]-\hat{\gamma}\,\frac{\hat{\psi}^2(d)}{2}\right\}, \tag{37}$$

where

$$\hat{\psi}(d)\equiv\mu^2\psi=\frac{3}{d^2}\left(\frac{1}{2}+\mathrm{Fr}^2-\frac{d^2}{2}-\frac{\mathrm{Fr}^2}{d}\right), \quad \hat{w}(d)=\frac{3}{d^4}[3\mathrm{Fr}^2-(1+2\mathrm{Fr}^2)d], \tag{38}$$

and $\hat{\gamma}=\gamma/a$. Equation 37 has been obtained under the usual hypotheses for solitary waves, that is: (i) we assume the flow is steady in the coordinate system moving with a constant Froude number $\mathrm{Fr}=V^*/\sqrt{gd_0^*}>0$, (ii) we assume all the variables to depend only on $\xi=(x-\mathrm{Fr}\,t)/\mu$, (iii) we consider the typical "Solitary wave" asymptotic conditions, that is:

$$Q,\phi,\psi\to 0, \quad d\to h, \quad \frac{\mathrm{d}d}{\mathrm{d}\xi}\to 0, \quad \frac{\mathrm{d}^2d}{\mathrm{d}\xi^2}\to 0, \quad \text{for } \xi\to\pm\infty.$$

By applying the square root to (37), two different ODEs can be found; each of them represents one half of the solitary wave (the positive root is the ascending part, while the negative one is descending). Equation 37 has to be solved with the initial condition

$$d(x=0)=h \tag{39}$$

until the crest of the solitary wave $d_{\max}$ is reached. Since the term

$$\Delta=3\left[\frac{\mathrm{Fr}^2}{2d^2}-\frac{1+2\mathrm{Fr}^2}{2d}-\frac{d}{2}+1+\frac{\mathrm{Fr}^2}{2}\right]-\hat{\gamma}\,\frac{\hat{\psi}^2(d)}{2} \tag{40}$$

has among its zeros the maximum value of the water depth $d_{\max}$ of the solitary wave and the still water level h, solving such an equation can give rise to numerical problems. These can be overcome by first modifying the initial condition as

$$d(x=0)=h+\varepsilon, \tag{41}$$

with $\varepsilon\ll 1$. Then an appropriate numerical tool has to be used. We have chosen the same algorithm implemented for the solution of the system of the DNSWEs [10]. Such a scheme automatically reduces to a standard DG method for the nonlinear system of ODEs

$$\frac{\mathrm{d}}{\mathrm{d}t}\mathbf{U}=\mathbf{S}(\mathbf{U}). \tag{42}$$

Once the solution for d has been found, the dimensional d^* can be obtained as $d^*=d_0^*d$. Hence, the other variables Q^*, ϕ^* and ψ^* can be computed. In particular, Q is given by (see ALB08):

$$Q=\mathrm{Fr}(d-1), \tag{43}$$

from which the dimensional flow rate

$$Q^*=d_0^*\sqrt{gd_0^*}\,Q. \tag{44}$$

We can compute ψ^* by using the solution for $\hat{\psi}$ given in (38). We get:

$$\psi^*=\psi_0^*\psi=\psi_0^*\frac{\hat{\psi}}{\mu^2}=\frac{d_0^*}{a}\hat{\psi}. \tag{45}$$

Finally, to compute ϕ^*, we use the following result:

$$\hat{\phi}\equiv\mu\phi=\sqrt{2\left\{3\left[\frac{\mathrm{Fr}^2}{2d^2}-\frac{1+2\mathrm{Fr}^2}{2d}-\frac{d}{2}+1+\frac{\mathrm{Fr}^2}{2}\right]-\hat{\gamma}\,\frac{\hat{\psi}^2(d)}{2}\right\}}, \tag{46}$$

and, finally, get:

$$\phi^* = \frac{\sqrt{g d_0^*}}{A^*}\hat{\phi} = \frac{d_0^*}{a}\sqrt{\frac{d_0^*}{g}}\hat{\phi}. \tag{47}$$

These formulations allow us to compute d as a function of the Froude number Fr (see (37)), instead of the maximum wave height. If $d_{\max}$ has to be assigned, a particular procedure has to be followed. Let us first recall that, if $\hat{\gamma} = 0$, it is $d_{\max} = \mathrm{Fr}^2$. Moreover, $d_{\max}$ is one of the roots of Δ in Eq. 40. Hence, $d_{\max}$ can be computed iteratively, by finding the Froude number which makes one of the roots of (40) equal to the desired $d_{\max}$. A starting value of Fr is given by the approximation for $\hat{\gamma} = 0$, i.e., $\mathrm{Fr} = \sqrt{d_{\max}}$.

The procedure to get the desired solitary wave initial condition is:

1. choose the desired solitary wave, i.e., assign $d_{\max}$;
2. compute the relative Froude number Fr;
3. solve (37) and get d^* for the ascending part of the solitary wave;
4. by symmetry compute d^* for the descending part;
5. compute Q^*, ψ^* and ϕ^* with Eqs. 44, 45 and 47.

With initial condition described above and still water depth $h^* = 1\mathrm{m}$ some numerical computations have been performed using 300 cells and periodic boundary conditions. In the top panel of Fig. 2, the total water depth is plotted for both solutions. The solid line represents the analytical solution, while the dotted line represents the 3rd order numerical solution after 2s. The dashed line, instead, shows the 3rd order numerical solution after a complete loop of the wave over the computational domain. The lower panel of the same Fig. 2, instead, gives the same illustration for the variable ψ^*. The match between the analytical and the numerical solutions for both variables is excellent, the two curves being visually superposed one to the others. Such a good agreement, which also testifies the good performances of the periodic boundary conditions, clearly illustrates the absence of any dissipative numerical effects. This is particulary remarkable for the variable ψ^*, which is strongly affected by the stiffness of the source terms.

4.2 Propagation of waves on a beach

The DNSWEs are here applied to study a case of one-dimensional wave propagation, i.e., that of solitary waves propagating over plane slopes. Simulations have been performed for solitary waves with different initial relative height $\epsilon = H_0^*/d_0^*$, propagating over various different slopes ranging from gentle to steep. Figure 3 gives the main details about the domain configuration, which consists of a constant-depth (d_0^*) region on the left and a sloping (s) region on the right. Coordinates are set such that the toe of the slope corresponds to $x = 0$. Solitary waves are generated over the constant-depth region and made propagate to the right.

In order to compare the model performances with a reliable and well-known benchmark for non-breaking waves propagating over a beach, we have reproduced the flow conditions described in Wei et al. [17]. Hence, four different slopes, $s = 1:100$, $1:35$, $1:15$ and $1:8$, have been used in the computations. On each slope, solitary wave of relative heights of $\epsilon = 0.2$ and $\epsilon = 0.3$ have been run (see Fig. 4).

It is here essential to recall (see `ALB08` for more details) that the solitary wave solution of the DNSWEs is different in shape from the classical solitary waves used to initialize BTEs models (see Fig. 4). [This fact is typical of the comparison between model equations which admit different permanent-form solitary wave solution (see, for example, [17]).] In particular the DNSWEs solitary wave is broader than the KdV one (see [18, Chap. 11] for details), the difference in breadth increasing with increasing nonlinearity (ϵ). This, obviously, induces shape differences for the entire propagation process which are product neither of the DNSWEs model propagation mechanism nor of the numerical computation.

In the top panel of Fig. 5 the DNSWEs wave solutions are plotted against the solutions computed by [17], see their Fig. 4, using their Fully Nonlinear Boussinesq Model, for $\epsilon = 0.2$ and $s = 1:35$ at different time steps ($t_1^* = 5.19s$,

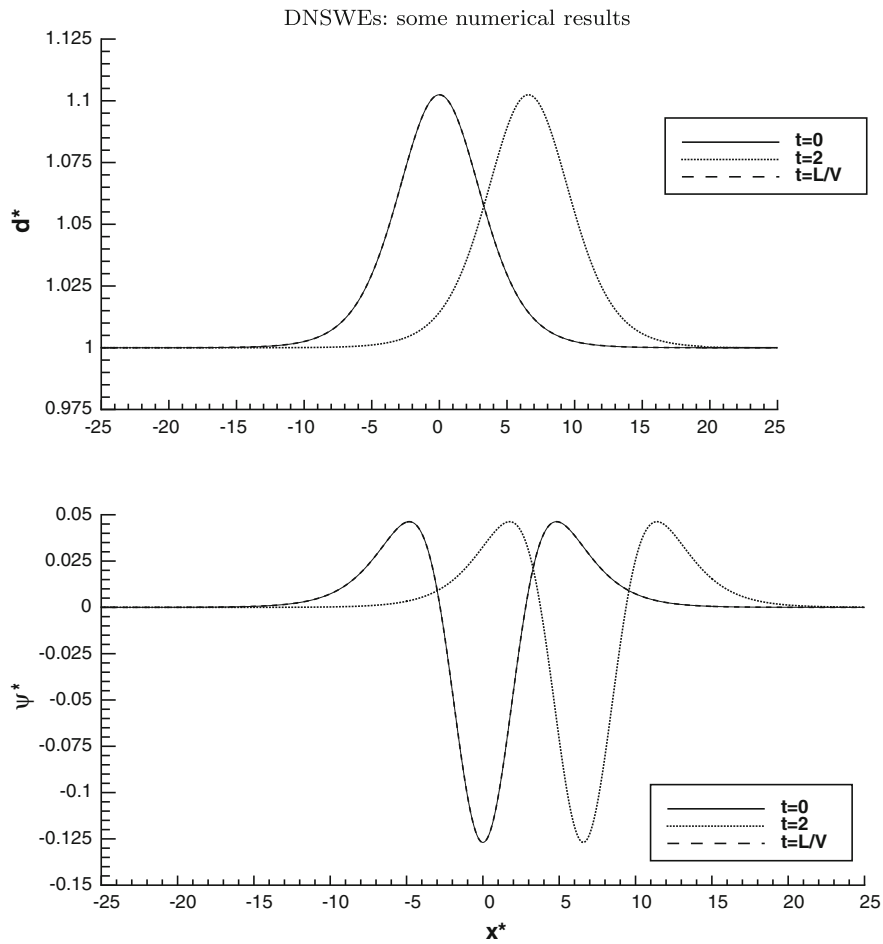

Fig. 2 Solitary wave on horizontal bed

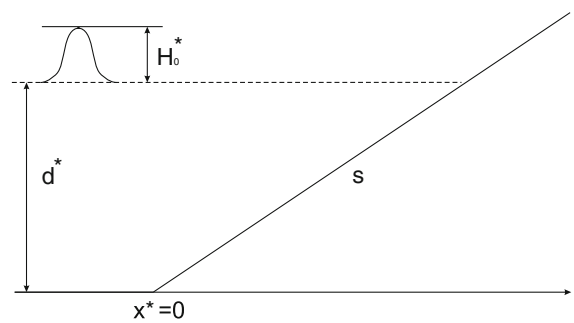

Fig. 3 Sketch of a solitary wave propagating on a beach

$t_2^* = 6.59s$, $t_3^* = 7.67s$ and $t_4^* = 8.28s$). [We set $t^* = 0$ when wave crests reach the toe of the slope $x^* = 0$, hence the possible reference to negative times.]

In the lower panel of the same figure similar wave solutions are shown for the case $\epsilon = 0.3$ and $s = 1{:}8$ at the times $t_1^* = -0.24s$, $t_2^* = 0.82s$, $t_3^* = 1.78s$ and $t_4^* = 2.18s$. The first profile to the left of both panels corresponds to waves about half way up the slope while the last of the top panel corresponds to the theoretical breaking points in fully nonlinear potential flow computations (no breaking occurs for the waves of the lower panel).

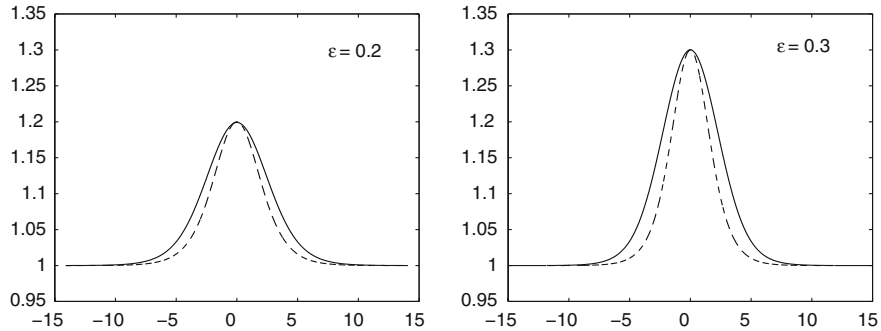

Fig. 4 Comparison between the DNSWEs solitary wave (*solid line*) and the KdV solitary wave (*dashed line*) for $\epsilon = 0.2$ (*left panel*) and $\epsilon = 0.3$ (*right panel*)

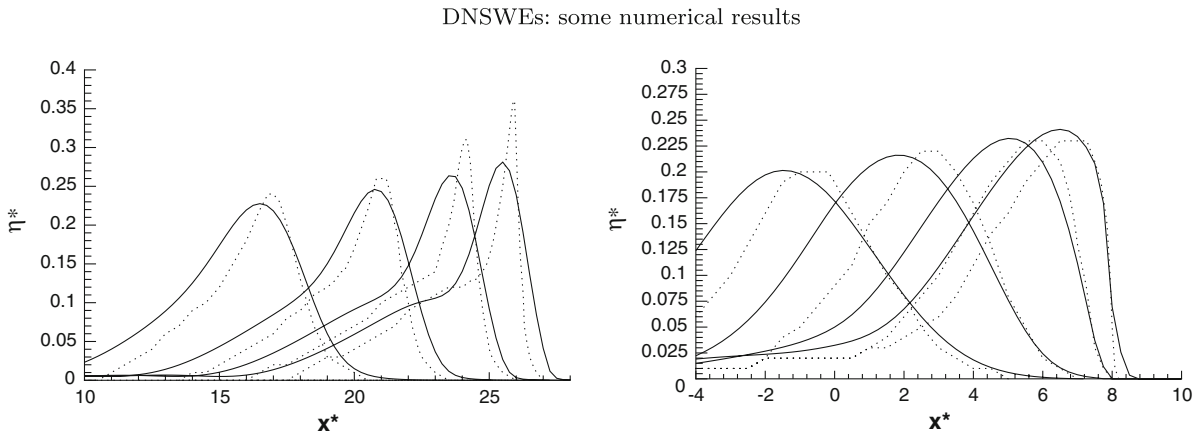

Fig. 5 Solitary waves on a beach. The numerical solution of the DNSWEs (*solid line*) and the fully nonlinear Boussinesq Model solution of [17] (*dashed line*, and adapted from Fig. 4 of their paper) are plotted at different times of evolution (from left to right). *Top panel* $\epsilon = 0.2$, $s = 1{:}35$. Evolution times are $t^* = 5.19s, 6.59s, 7.67s, 8.28s$. *Bottom panel* $\epsilon = 0.3$, $s = 1 : 8$. Evolution times are $t_1^* = -0.24s, 0.82s, 1.78s, 2.18s$

From these figures, it is evident that, apart from the predictable difference in wave shape (DNSWEs waves are broader), there is a good agreement between positions of the wave fronts predicted by our model and the ones given by [17]. Hence, the wave crest trajectories are in agreement.

For the case $\epsilon = 0.3$ and $s = 1{:}8$, characterized by an Ursell number ϵ/s^2 of about 20 and such that no deformations of the wave tail appear, also the shoaling properties are comparable with those of the Fully Nonlinear Boussinesq Model of [17].

Rather different is the case $\epsilon = 0.2$ and $s = 1{:}35$, characterized by an Ursell number of about 250 for which nonlinearities and deformation of the wave tail are important, for which the DNSWEs solution displays a rather important (about 15% at breaking) undershoaling with respect to the solution of [17]. This contrasts with the typical behaviour of weakly nonlinear BTEs which, not accounting for high-order contributions in the dispersive parameter ($\mu = kh$ or s), usually produce major overshoaling with respect to fully nonlinear solvers (see [17] for examples). The reasons for such an undershoaling have to be sought both in the specific chosen DNSWEs (weakly nonlinear), in the shape of the initial condition solution of the DNSWEs and in the numerical method used for the solution (finite-volume techniques, using the weak form of the differential problem, allow for discontinuous solution). More analysis is required in this respect aimed at both evaluating the shoaling properties of the model equations and the dissipative features of the numerical solver. These can be calibrated by multiplying the higher-order differential

contribution to the momentum equation (of the type $(.)_{xxt}$ in our case) by a constant coefficient. Both analyses are ongoing and details will be reported in a forthcoming manuscript.

However, we find it very pleasing to see that a weakly nonlinear DNSWEs model, which contains no calibration or tuning parameter, captures well the most significant properties of the solution reported by [17], even when undershoaling occurs.

5 Conclusions

A brief, but complete, account on the theory of the DNSWEs of ALB08 has been provided along with a more detailed description of the adaptation of the high-order, finite-volume technique by [10] to the solution of the mentioned differential system. Subsequently, some preliminary results on the numerical solution of the DNSWEs have been proposed and illustrated. Analytical and numerical benchmarks have been chosen for this preliminary analysis which reveals some of the potentials of solving a dispersive–hyperbolic system by means of methods typically used for hyperbolic sets of nonlinear equations. Work is ongoing to make the model at hand more easily applicable to computations of practical use.

Acknowledgements This work was partially supported by the European Union through the INTAS Grant No. 06-1000013-9236 and by the Italian Ministero dei Trasporti within the framework of the "Programma di Idrodinamica Navale INSEAN 2007–2009". The three anonymous Reviewers are thanked for their constructive criticism which helped improve the clarity of our description. The paper is dedicated to Prof. Howell Peregrine who provided fundamental inspiration and guidance: the analyses presented here are an indirect outcome of his enthusiasm and dedication to the modeling of nearshore flows.

References

1. Peregrine DH (1967) Long waves on a beach. J Fluid Mech 32:353–365
2. Hibberd S, Peregrine DH (1979) Surf and run-up on a beach: a uniform bore. J Fluid Mech 95:323–345
3. Bernetti R, Toro EF, Brocchini M (2003) An operator-splitting method for long waves. In: Proc Long Waves Symposium vol. 1, pp. 49–56. Thessaloniki, Greece
4. Briganti R, Brocchini M, Bernetti R (2004) An operator-splitting approach for Boussinesq-type equations. In: GIMC 2004, XV Convegno Italiano di Meccanica Computazionale—AIMETA
5. Erduran KS, Ilic S, Kutija V (2005) Hybrid finite-volume finite-difference scheme for the solution of Boussinesq equations. Int J Numer Methods Fluids 49(11):1213–1232
6. Cienfuegos R, Barthelemy E, Bonneton P (2006) A fourth order compact finite volume scheme for fully nonlinear and weakly dispersive Boussinesq-type equations. Part I: model development and analysis. Int J Numer Methods Fluids 51(11):1217–1253
7. Antuono M, Liapidevski V, Brocchini M (2008) Dispersive Nonlinear Shallow-Water Equations. Stud Appl Math 122:1–28
8. Veeramony J, Svendsen IA (2000) The flow in surf-zone waves. Coast Eng 39(2–4):93–122
9. Bellotti G, Brocchini M (2002) On using Boussinesq-type equations near the shoreline: a note of caution. Ocean Eng 29(12):1569–1575
10. Dumbser M, Enaux C, Toro EF (2008) Finite volume schemes of very high order of accuracy for stiff hyperbolic balance laws. J Comput Phys 227(8):3971–4001
11. Dumbser M, Käeser M (2007) Arbitrary high order non-oscillatory finite volume schemes on unstrucutred meshes for linear hyperbolic systems. J Comput Phys 221:693–723
12. Harten A, Engquist B, Osher S, Chakravarthy S (1987) Uniformly high order essentially non-oscillatory schemes, III. J Comput Phys 71: 231–303
13. Stroud AH (1971) Approximate calculation of multiple integrals. Prentice-Hall Inc, Englewood Cliffs
14. Bermúdez A, Vázquez-Cendón ME (1994) Upwind methods for hyperbolic conservation laws with source terms. Comput Fluids 23: 1049–1071
15. Castro M, Gallardo J, Parés C (2006) High order finite volume schemes based on reconstruction of states for solving hyperbolic systems with nonconservative products. Application to shallow water systems. Math Comput 75(255):1103–1134
16. Parés C, Castro M (2004) On the well-balanced property of Roe's method for nonconservative hyperbolic systems. Applications to shallow water systems. ESAIM: M2AN 38(5):821–852
17. Wei G, Kirby JT, Grilli ST, Subramanya R (1995) A fully nonlinear Boussinesq model for surface waves: I. Highly non-linear, unsteady waves. J Fluid Mech 294:71–92
18. Mei CC (1983) The applied dynamics of ocean surface waves. Wiley, New York